RSC Advances

ROYAL SOCIETY OF CHEMISTRY

www.rsc.org/advances

Ab-initio investigation on the stability of H-6 Carbon

Zacharias G. Fthenakis[a]

A few years ago H-6 Carbon had been proposed as an all sp^2 three-dimensional Carbon allotrope, with mechanical properties comparable to graphene. However, results on the stability of H-6 Carbon presented in the literature are rather contradictory and confusing, and it is not yet clear if this hypothetical allotrope is stable or not. Studying systematically the stability of H-6 Carbon, using ab-initio density functional theory and phonon band structure calculations, we show that H-6 Carbon is unstable, converted spontaneously to diamond. According to our findings, the instability mechanism is not the same with that of compressed rhombohedral graphite, but is related to the synergetic action of the interchain interactions of the parallelly arranged zig-zag chains and the strain induced by the 60^o rotation (with respect to graphite) of the interconnected zig-zag chains. This synergetic action eliminates the barrier provided by the intrachain interactions, causing the transition of H-6 Carbon to diamond.

1 Introduction

The scientific community was always interested in Carbon allotropes. This is not surprising, since it is well known the flexibility of Carbon to form single, double and triple bonds, thus allowing (in principle) the formation of several networks and structures with different bonding and properties [1–10]. H-6 Carbon is such an hypothetical three-dimensional all sp^2 structure, which was proposed two decades ago [11], as another Carbon allotrope. It consists of arrays of parallelly arranged zig-zag chains, which are rotated with each other by 60^o (or 120^o), as shown in Fig. 1(a).

Tamor and Hass [11], who first proposed and studied H-6 Carbon using a Tight Binding (TB) approach, found that H-6 Carbon is stable. A year later, Liu et al [12], using density functional theory (DFT) in the local-density approximation (LDA) level, found that H-6 Carbon is unstable. On the other hand, Winkler et al [13], Rignanese and Charlier [14] and recently Bon Zhang [15], using ab-initio DFT calculations reported that H-6 Carbon is stable. All these results are rather confusing, and it is not yet clear if H-6 Carbon is stable or not. It is worth noting, however, that none of the above calculations [13–15] is accompanied by a phonon band structure (or any other) calculation, which would ensure that the optimized structure found corresponds to a true energy minimum and not to a saddle point of the potential energy surface (PES).

In the present study we try to shed light on the issue of the stability of H-6 Carbon. We systematically optimize H-6 Carbon performing ab-initio DFT calculations with two different functionals, and different number of k-grid points and mesh cutoff values and we found that independent of them optimizations lead either to diamond or H-6 Carbon structure. Performing energy calculations with both functionals along a transition pathway converting the optimized H-6 Carbon structure to diamond, as well as phonon band structure calculation for the optimized H-6 Carbon, we show that H-6 Carbon is unstable. Contrary to this result, we show that the TB method, which was used by Tamor and Hass [11] to optimize the H-6 Carbon structure, finds an energy barrier along that transition pathway. As we explain, this barrier is overestimated due to the cutoff function used, and the main reason for its existence is the incorrect description (or the absence) of interchain interactions. Moreover, performing several optimization calculations for the H-6 Carbon structures under 10% tensile strain, we show that increasing the distance between the parallelly arranged zig-zag chains, does not stabilize the structure, concluding that the instability mechanism of H-6 Carbon is different from that of compressed rhombohedral graphite [16], as proposed by Liu et al [12]. Performing energy calculations along the transition path which converts a graphitic-like structure (which could be obtained if the arrays of zig-zag chains of H-6 Carbon were not rotated) to diamond, and combining these results with the corresponding results obtained from the calculations on H-6 Carbon using DFT/LDA and TB methods, we find that the instability mechanism of H-6 Carbon is related to the synergetic action of the interchain interactions of the parallelly arranged zig-zag chains and the strain induced by the 60^o rotation (with respect to graphite) of the interconnected zig-zag chains. This synergetic action eliminates the barrier provided by the intrachain interactions, making H-6 Carbon unstable.

2 The Method

As already mentioned, H-6 Carbon is a periodic structure composed of arrays of parallelly arranged zig-zag Carbon chains. Those layers are rotated with each other by 60^o (or 120^o). The structure is shown in Fig. 1(a), where different colors show different layers of those zig-zag chains. The Bravais lattice is hexag-

[b] Institute of Electronic Structure and Laser, FORTH, P.O. Box 1527, 71110 Heraklio, Crete, Greece; E-mail: fthenak@iesl.forth.gr

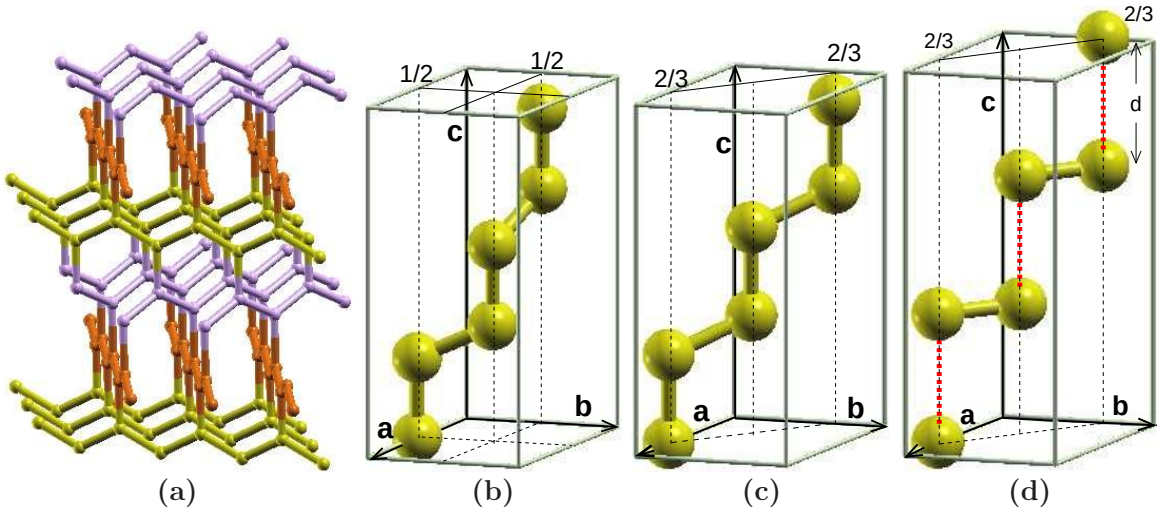

Fig. 1 (Color online). H-6 Carbon structure and the unit cells of the homeomorphic structures H-6, diamond and rhombohedral graphite. (a) Side view of H-6 Carbon. Different colors indicate different layers of parallelly arranged zig-zag Carbon chains, rotated by 60^o (or 120^o). (b) The unit cell of H-6 Carbon. (c) The unit cell of diamond. (d) The unit cell of rhombohedral graphite. Red dashed lines indicate interlayer distances.

onal, defined by the unit cell vectors

$$\mathbf{a} = a\left(\frac{1}{2}, -\frac{\sqrt{3}}{2}, 0\right), \quad \mathbf{b} = a\left(\frac{1}{2}, \frac{\sqrt{3}}{2}, 0\right) \quad \text{and} \quad \mathbf{c} = c(0,0,1). \tag{1}$$

For the initial values of a and c for our optimizations, we adopt the values reported by Zhang[15], i.e. $a = 2.618$ Å and $c = 6.295$ Å. The unit cell, which is shown in Fig. 1(b), contains six C atoms with fractional coordinates (1/2, 0, 0), (1/2, 0, δ), (1/2, 1/2, 1/3), (1/2, 1/2, 1/3+δ), (0, 1/2, 2/3) and (0, 1/2, 2/3+δ) , where $\delta = 0.228$. These positions are identical with those used by Zhang[15].

The H-6 Carbon structure is optimized using the DFT method as implemented in the SIESTA code[17]. All the energy calculations used in the present work have been performed using this method. For the exchange and correlation functional we utilize the LDA Ceperley-Adler (CA) functional[18] as parametrized by Perdue and Zunger[19], and the generalized gradient approximation (GGA) Perdue-Burke-Ernzerhof (PBE) functional[20]. For the pseudopotential of C we utilize the norm-conserving Troullier-Martins pseudopotentials[21] in the Kleinman-Bylander factorized form[22]. The basis for the wavefunction expansion in real space is an atomic-like double-zeta basis with polarization orbitals. In order to control the effect of the finite number of k-points of the reciprocal space, as well as the finite value of the mesh cutoff energy for the determination of charge densities and potentials, on the optimized geometry and total energy, we performed several calculations combining increasing number of k-grid points with increasing mesh cutoff values for both functionals. Thus, for the k-point grid we used the Monkhorst - Pack scheme[23] with $16\times16\times7$, $24\times24\times10$ and $32\times32\times14$ points and for the mesh cutoff we used the values 100, 200 and 300 Ry. For the optimizations we use the conjugate gradient method. Optimizations include not only relaxation of atomic positions, but also relaxation of the lattice vectors. The structure is assumed to be optimized if the maximum atomic force and the maximum stress component become smaller than 0.005 eV/Å and 0.01 GPa, respectively.

H-6 Carbon structure is homeomorphic to diamond and rhombohedral graphite, which means that from the topological point of view they are the same. Both diamond and rhombohedral graphite can be considered as forming a hexagonal lattice, with the unit vectors having the same form as in H-6 Carbon (see Eq. 1). For diamond $a = 2\sqrt{2/3}a_{0,dia}$ and $c = 4a_{0,dia}$, where $a_{0,dia}$ is the bond length of diamond. The fractional coordinates of the six atoms contained in its unit cell are (2/3, 0, 0), (2/3, 0, 3/12), (1/3, 1/3, 1/3), (1/3, 1/3, 7/12), (0, 2/3, 2/3) and (0, 2/3, 11/12). For rhombohedral graphite $a = \sqrt{3}a_{0,gr}$ and $c = 3d$, where $a_{0,gr}$ is the bond length of graphene and d is the interlayer separation distance. The fractional coordinates of the six atoms contained in its unit cell are (2/3, 0, 0), (2/3, 0, 1/3), (1/3, 1/3, 1/3), (1/3, 1/3, 2/3), (0, 2/3, 2/3) and (0, 2/3, 1). The unit cells of diamond and rhombohedral graphite are shown in Figs. 1(c) and (d), respectively.

Since H-6 Carbon, rhombohedral graphite and diamond are homeomorphic with each other, there is a continuous transformation converting H-6 Carbon to diamond or rhombohedral graphite and vice versa. The simplest transition path, which linearly converts H-6 Carbon to diamond is defined by the unit cell vectors of Eq. 1, with

$$a = a_{H6} + \lambda(a_{dia} - a_{H6}) \quad \text{and} \quad c = c_{H6} + \lambda(c_{dia} - c_{H6}), \tag{2}$$

(where a_{H6} and c_{H6} are the values of a and c for H-6 Carbon, and a_{dia} and c_{dia} for diamond), and the fractional coordinates $(1/2+\lambda/6, 0, 0)$, $(1/2+\lambda/6, 0, \delta+\lambda(1/4-\delta))$, $(1/2-\lambda/6, 1/2-\lambda/6, 1/3)$, $(1/2-\lambda/6, 1/2-\lambda/6, 1/3+\delta+\lambda(1/4-\delta))$, $(0, 1/2+\lambda/6, 2/3)$ and $(0, 1/2+\lambda/6, 2/3+\delta+\lambda(1/4-\delta))$ of the six atoms contained in the unit cell, where $0 \le \lambda \le 1$. For $\lambda = 0$, the structure is the H-6 Carbon, while for $\lambda = 1$, it is the diamond structure. We will calculate the energy of H-6 Carbon along this transformation path, to show that H-6 Carbon is unstable.

3 Results and Discussion

3.1 Is H-6 Carbon stable?

The optimizations of the initial H-6 Carbon structure described above leads either to H-6 Carbon or diamond, without any convergence trend for increasing number of k-grid points or mesh cutoff value. The total energy per atom, as well as the optimized structures found for each case are presented in Table 1 of the Electronic Supplementary Information (ESI). However, for increasing number of k-grid points or mesh cutoff value in the range used, the accuracy of the calculations is not affected by more than 1 meV/atom, which means that, separately, the results which are referred to H-6 Carbon and those referred to diamond are converged.

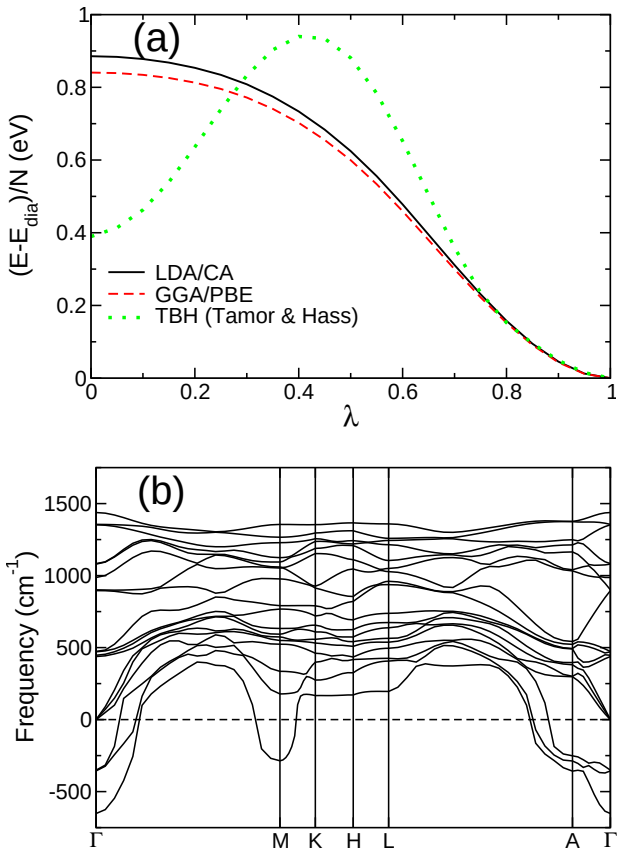

Fig. 2 (a) Total energy per atom of H-6 Carbon with respect to that of diamond versus λ, calculated using (i) the LDA/CA functional, a Monkhorst-Pack k-grid of 16x16x7 points and a mesh cutoff value of 100 Ry (black solid line), (ii) the GGA/PBE functional, a Monkhorst-Pack k-grid of 16x16x7 points and a mesh cutoff value of 300 Ry (red dashed line) and (iii) the TB approach with FNN interactions only, used by Tamor and Hass[11] for their calculation on H-6 Carbon (green dotted line). (b) Phonon band structure of H-6 Carbon along ΓMKHLAΓ points.

In order to clarify if the optimized H-6 Carbon structure found corresponds to a true energy minimum or a saddle point of the PES, we calculate the total energy per atom along the transition pathway described in section 2, which connects H-6 Carbon with diamond, for increasing λ values from 0 to 1, with a 0.05 step. The results for both functionals (LDA/CA and GGA/PBE) are shown in Fig. 2(a). As we can see, the total energy monotonically decreases as a function of λ for both functionals, and consequently, there is not an energy barrier in the PES between H-6 Carbon and diamond. Similar results has been reported by Liu et al[12]. Therefore, according to the DFT calculations, the optimized H-6 Carbon structure found, does not correspond to a true energy minimum.

We verify the above result performing a phonon band structure calculation for the optimized H-6 Carbon structure which was found using the LDA/CA functional with a 16x16x7 Monkhorst-Pack grid of k-points and a 100 Ry mesh cutoff value. We used the vibra utility of siesta code, with a 5x5x3 supercell containing 450 atoms and a 0.02Å displacement of each atom of the central unit cell along $\pm x$, $\pm y$ and $\pm z$ directions. The phonon dispersion relation was calculated along the path ΓMKHLAΓ, where the high symmetry points Γ, M, K, H, L and A of the reciprocal space are defined in fractional coordinates as Γ=(0, 0, 0), M=(1/2, 1/2, 0), K=(2/3, 1/3, 0), H=(2/3, 1/3, 1/2), L=(1/2, 1/2, 1/2) and A=(0, 0, 1/2). The obtained phonon band structure is shown in Fig. 2(b), where we can see the existence of negative frequencies ω, which prove that indeed H-6 structure is unstable.

Interestingly, on the other hand, if we calculate the energy along the same transition path using the TB method which was used by Tamor and Hass[11], then it appears an energy barrier, as shown in Fig. 2(a) (green dotted line), indicating that H-6 Carbon might be stable according to the TB calculation.

3.2 Understanding the TB failure

The TB Hamiltonian used by Tamor and Hass utilizes the Slater-Koster[24] parameters of Tománek and Louie[25] considering only first nearest neighbour (FNN) interactions (i.e. SNN interactions are not taken in account). More details of this TB method are presented in the ESI. To eliminate SNN interactions, Tamor and Hass used a cutoff function $f_c(d)$ of the interatomic distance d, which is $f_c(d) = 1$ for $d < 1.7$Å, $f_c(d) = 0$ for $d > 2.4$Å and for 1.7 Å$< d <$ 2.4 Å, f_c decays smoothly from 1 to 0. Such a decay introduces unphysical interactions between atoms with 1.7 Å$< d <$ 2.4 Å and may lead to erroneous results.

For $d <$ 2.4 Å, the interatomic distances which can be identified for H-6 Carbon are (i) d_{12} and $d_{12'}$ between FNN of the same zig-zag chain, (ii) d_{13} between atoms connecting rotated zig-zag chains and (iii) d_{14} and $d_{14'}$ between atoms belonging to neighbouring zig-zag chains of the same array, as shown in Fig. 3(a) with blue, green (solid) and red (dashed) lines, respectively. Along the transition pathway connecting H-6 with diamond, $d_{12} = d_{12'}$, $d_{14} = d_{14'}$ for $\lambda = 0$ and $d_{14} < d_{14'}$ for $\lambda > 0$. d_{12}, d_{13} and d_{14} varies as a function of the parameter λ, as shown in Fig. 3(b). d_{12} and d_{13} increase from 1.47 and 1.45 Å, respectively, to 1.53 Å, and d_{14} decreases from 2.37 to 1.53 Å. Thus, d_{14} falls in the range $[1.7, 2.4]$ Å, and therefore, 1-4 interactions are influenced by the unphysical effects of the f_c function.

Using the f_c function of Tamor and Hass, the barrier of the cohesive energy U_{coh} along the transition pathway converting H-6 Carbon to diamond is ≈ 0.6 eV, as shown in Fig. 2(a). If instead of this f_c function we use the sharp function $f_c(d) = 1 - \theta(d - d_0)$, (where $\theta(d - d_0) = 0$ if $d < d_0$ and 1 if $d > d_0$), for $d_0 = 1.7$ Å and

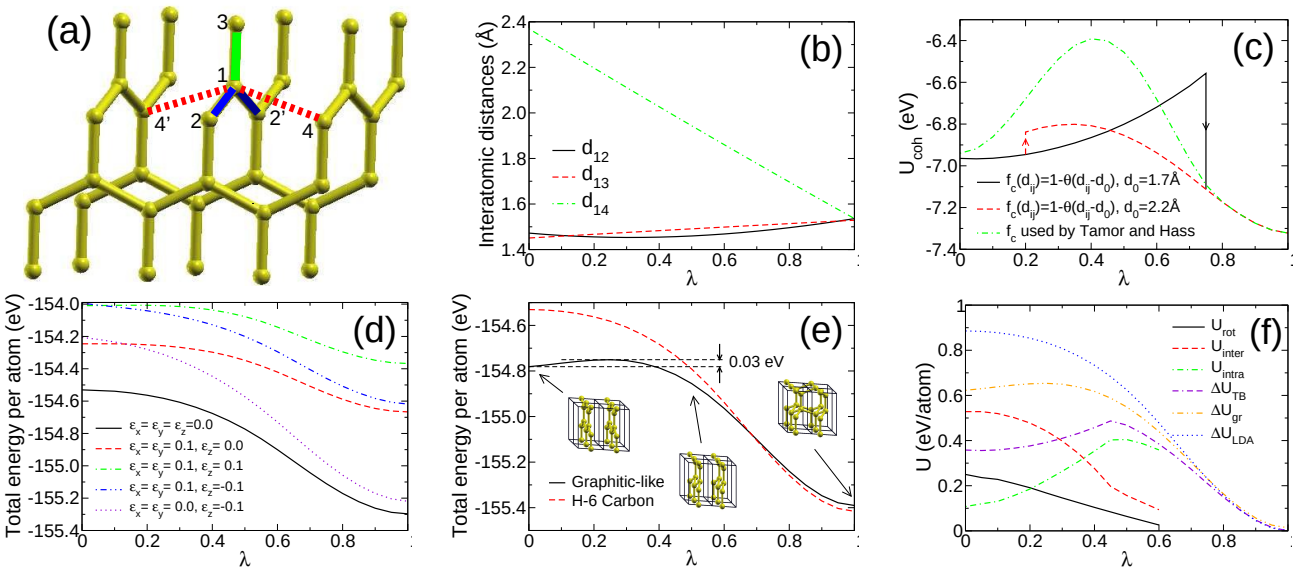

Fig. 3 (Color online) (a) Interatomic distances in H-6 Carbon. (b) Interatomic distances along the transition pathway. (c) Cohesive energy along the transition pathway according to the TB method of Tamor and Hass[11], using different cutoff functions, (d) Energy per atom along the transition pathway converting stretched H-6 Carbon to diamond for several strain conditions. (e) Energy per atom along the transition pathway converting the graphitic-like structure to hexagonal diamond. The energy per atom of H-6 Carbon for the corresponding transition path converting it to diamond is shown for comparison. Snapshots of the graphitic-like structure for $\lambda = 0$, 0.5 and 1 are shown. (f) Energy contributions U_{rot}, U_{inter}, U_{intra}, as well as their combinations ΔU_{TB}, ΔU_{gr} and ΔU_{LDA}, as a function of λ.

$d_0 = 2.2$Å, (the former ignores the 1-4 interaction for $d_{14} > 1.7$ Å and the latter for $d_{14} > 2.2$ Å), then the barrier seems to be much smaller, as shown in Fig. 3(c). Based on this, it seems that a more reliable estimation of the energy along that transition pathway is obtained using the combination of the lower energy branches of the energy curves of Fig. 3(c), i.e for $d_0 = 1.7$ Å (black solid line) and $d_0 = 2.2$ Å (red dashed line) up to their crossing point. This is equivalent to use a cutoff function with $d_0 \approx 1.9$ Å. This TB estimation provides an energy barrier of ≈ 0.1 eV, which seems to be more reliable. Consequently, the unphysical effects, introduced by the cutoff function in the TB Hamiltonian used by Tamor and Hass[11], are a source of a large error for the energy barrier height.

Still, however, the energy barrier remains in the TB calculation, in contrast to the DFT results. Despite possible sources of error, like the transferability of the Slater-Koster parameters, the form of the repulsive potential and the cutoff function f_c, the most important factor causing this discrepancy is the incorrect description (and/or the absence) of SNN interactions and especially the week 1-4 $pp\sigma$ interchain interactions between the $p_\perp$-orbitals, which are perpendicular to the parallelly arranged zig-zag chains. This will be clear in the next subsection.

3.3 Which factors are responsible for the instability?

Liu et al[12] noted that the instability mechanism of H-6 Carbon might be similar to that of rhombohedral graphite at short interlayer distances, since the interatomic distance $d_{14} = 2.37$ Å of H-6 Carbon is comparable to the interlayer separation range (between 2.1 and 2.3 Å, according to Fahy et al[16]) at which the transformation of rhombohedral graphite to diamond is favoured.

However, the first indication that the instability mechanism of H-6 Carbon might be different from the one converting rhombohedral graphite to diamond, is that the in-layer C-C bonds of the compressed rhombohedral graphite normal to the graphitic layers are tilted towards that direction much earlier before its transition to diamond[16,26], causing a buckling of the graphitic layers. In H-6 Carbon the zig-zag chains do not buckle and atoms 1 and 4 of Fig. 3(a) remain coplanar with their FNN. Therefore, if the instability mechanism of H-6 Carbon was the same with that of rhombohedral graphite under compression, then the zig-zag chains of H-6 Carbon should be buckled.

$\varepsilon_x = \varepsilon_y$	ε_z	a	c	d_{12}	d_{13}	d_{14}
0.0	0.0	2.624	6.363	1.472	1.455	2.368
0.1	0.0	2.886	6.363	1.582	1.459	2.593
0.1	0.1	2.886	6.999	1.539	1.577	2.615
0.1	-0.1	2.886	5.727	1.583	1.308	2.559
0.0	-0.1	2.624	5.727	1.380	1.310	2.340

Table 1 Unit cell vector lengths (a and c) and bond lengths (d_{12}, d_{13}, d_{14}) in Å units of H-6 Carbon under strain (ε_x, ε_y, ε_z) without optimization.

Assuming, however, that the instability mechanism of H-6 Carbon is the same with that of compressed rhombohedral graphite, then H-6 Carbon would be stabilized if d_{14} was increased, as it happens with rhombohedral graphite. To increase d_{14}, we strained (by stretching and/or compression) the optimized H-6 Carbon structure, and we optimized the strained structures again. We tried four different strain cases, which increase d_{14}, namely (i) $\varepsilon_x = \varepsilon_y = 0.1$, (ii) $\varepsilon_x = \varepsilon_y = \varepsilon_z = 0.1$, (iii) $\varepsilon_x = \varepsilon_y = 0.1$ and $\varepsilon_z = -0.1$ and (iv) $\varepsilon_z = -0.1$, where ε_x, ε_y and ε_z is the strain along x, y and z direction, respectively. The lengths a and c of the unit cell vectors **a**, **b** and **c** of Eq. 1, as well as the bond lengths d_{12}, d_{13} and

d_{14} for each case are presented in Tab. 1. As we can see, in all cases the interatomic distance d_{14}, which is almost equal to the interchain separation, is longer than 2.3 Å. For such an interlayer separation distance, rhombohedral graphite does not turn into diamond[16,26]. However, optimizing the strained structures (i.e. optimizing the atomic positions for constant a and c values) using the LDA/CA functional, the optimum structure found for cases (iii) and (iv) was a strained diamond structure, but for the cases (i) and (ii), optimization stucks again in the unstable H-6 Carbon structure. Calculating, further, the energy along the corresponding transition pathway described in section 2, for all cases, we did not find any barrier, as shown in Fig. 3(d), concluding that the strained H-6 Carbon is again unstable. Consequently, tensile strain can not stabilize H-6 Carbon structure, (as it would happened in rhombohedral graphite) and, therefore, the instability mechanism of H-6 Carbon is different from that of compressed rhombohedral graphite.

In order to understand which factors are responsible for the H-6 Carbon instability, we consider an hypothetical graphitic-like structure, which is formed by the arrays of the parallelly arranged zig-zag chains of H-6 Carbon without any rotation, and we perform energy calculations along the transition pathway which converts it to diamond. The unit cell of this structure is defined by the unit cell vectors $\mathbf{a}' = \mathbf{a}$, $\mathbf{b}' = \mathbf{b}$ and $\mathbf{c}' = 2/3\mathbf{c}$, where $\mathbf{a}$, $\mathbf{b}$ and $\mathbf{c}$ are defined in Eq. 1, with a and c defined in Eq. 2. It contains only the first four atoms of H-6 Carbon, with positions which are defined by the fractional coordinates $(1/2+\lambda/6, 0, 0)$, $(1/2+\lambda/6, 0, (3/2)[\delta+\lambda(1/4-\delta)])$, $(1/2-\lambda/6, 1/2-\lambda/6, 1/2)$ and $(1/2-\lambda/6, 1/2-\lambda/6, (3/2)[1/3-\delta+\lambda(1/4-\delta)])$. The only difference between H-6 Carbon and this graphitic-like structure is the rotation of the zig-zag chains. It is worth noticing that the structure obtained for $\lambda = 1$ is not the common diamond, but the hexagonal diamond (also called *lonsdaleite*), which is very close energetically to the common diamond.

In Fig. 3(e), we present the energy of this graphitic-like structure along the transition pathway which converts it to hexagonal diamond, with snapshots of the structure for $\lambda = 0$, 0.5 and 1. For comparison we also present in the same figure the corresponding energy of H-6 Carbon along the transition pathway which converts it to diamond. As we can see, there is a 0.03 eV barrier per atom, which would stabilize the graphitic-like structure, and ensures that this graphitic-like structure does not spontaneously convert to hexagonal diamond. Obviously, the graphitic layers at the interlayer distance $d_{14} = 2.368$ Å of H-6 Carbon are repelled and this can explain the large value of d_{12} in comparison with the graphitic bond length. 1-2 and 1-2′ bonds are elongated in order to accommodate the stress of the parallelly arranged zig-zag chains.

It is worth noting that as in the case of H-6 Carbon (and contrary to rhombohedral graphite), the optimized graphitic-like structure, (without any optimization of the unit cell vectors), does not buckle. This behaviour for both cases is probably due to the relative arrangement of these layers, which is different from that of rhombohedral graphite and it seems that it does not favour buckling, thus strengthening the conclusion that different mechanisms govern the instability of H-6 Carbon and the conversion of rhombohedral graphite to diamond. This graphitic-like structure becomes unstable, turning into hexagonal diamond, only for $d_{14} < 2.15$ Å, (which corresponds to $\lambda \geq 0.25$).

According to the local atomic environment model, which have been successfully used to accurately predict the energy of graphene flakes[27], the energy of graphene-based structures is a sum of energy contributions depending on the local atomic environment of each atom of the structure. Based on this model we may consider that the total energy per atom ΔU_{LDA} of H-6 Carbon with respect to that of diamond according to the DFT/LDA calculation (i.e. $\Delta U_{LDA} = U_{H-6} - U_{dia}$, where U_{H-6} and U_{dia} are the total energies per atom of the H-6 Carbon structure and diamond, respectively, calculated using the DFT/LDA method), is a sum of three contributions; (i) the contribution of the intrachain interactions U_{intra}, representing (a) the strong interactions between the sp^2 orbitals and (b) the week ppπ interactions between the $p_\perp$ orbitals of a single graphitic-like sheet of the above mentioned graphitic-like structure, (ii) the contribution of the interchain interactions U_{inter}, representing the week ppσ and ppπ interactions between the $p_\perp$ orbitals of the neighbouring zig-zag chains, which are parallelly arranged, and (iii) the contribution of the strain induced by the rotation of the zig-zag chains U_{rot} with respect to the graphitic-like sheet, i.e. $\Delta U_{LDA} = U_{intra} + U_{inter} + U_{rot}$. The corresponding energy difference $\Delta U_{gr} = U_{gr} - U_{dia}$, where U_{gr} is the total energy per atom of the graphitic-like structure presented above, should be the sum of U_{intra} and U_{inter}, since the only difference between the graphitic-like structure and the H-6 Carbon structure is the rotation of the zig-zag chains. Thus, $\Delta U_{gr} = U_{intra} + U_{inter}$. Moreover, the cohesive energy difference $\Delta U_{TB} = U_{H-6}^{(TB)} - U_{dia}^{(TB)}$ of H-6 Carbon with respect to the diamond obtained using the modified TB method (i.e. using the sharp cutoff function with $d_0 = 1.9$ Å) presented in the previous section should be the sum of U_{intra} and U_{rot}, since the week SNN interactions between $p_\perp$ orbitals of the parallelly arranged zig-zag chains are not taken in account in the TB calculation, i.e. $\Delta U_{TB} = U_{intra} + U_{rot}$. Based on these three energy expressions, one may estimate the contributions U_{intra}, U_{inter} and U_{rot}, using the relations $U_{intra} = \Delta U_{TB} + \Delta U_{gr} - \Delta U_{LDA}$, $U_{inter} = \Delta U_{LDA} - \Delta U_{TB}$ and $U_{rot} = \Delta U_{LDA} - \Delta U_{rot}$. Based on these expressions, the values of U_{intra}, U_{inter} and U_{rot} along the transition pathway converting H-6 Carbon to diamond, in the range $0 \leq \lambda \leq 0.6$ are presented in Fig. 3(f). We do not present the corresponding U_{intra}, U_{inter} and U_{rot} values for $\lambda > 0.6$, because the energy separation in rotation, intrachain and interchain contributions looses its meaning as the structure is converted to diamond. Obviously, however, all three contributions become zero at $\lambda = 1$. For $0 \leq \lambda \leq 0.6$, where the structure keeps having the geometrical features of H-6 Carbon, (thus allowing the separation of energy to those three parts), we can see that U_{inter} and U_{rot} decrease as a function of λ, thus favoring the conversion of H-6 Carbon to diamond, but U_{intra} initially increases and then decreases, separating H-6 Carbon and diamond with a barrier. This barrier can not be eliminated with the sole combination of either U_{rot} or U_{inter} with U_{intra}, resulting in the barriers which appear in the ΔU_{TB} and ΔU_{gr}. However, the synergetic action of both the rotation and intrachain contribu-

tion eliminate the barrier provided by the intrachain contribution, making H-6 Carbon unstable.

Obviously, the rotation contribution can not be eliminated in the H-6 Carbon structure, however it can be reduced for other structures of the H-n family, (i.e. structures containing rotated by 60^o zig-zag ribbons, instead of just zig-zag chains). Due to this reduction, other structures of the H-n family might be stable. On the other hand, the interchain contribution could in principle be reduced under tensile strain, but as we have already seen for the four cases we have studied, the strain should be more than 10% to have a possibility to stabilize the structure.

4 Conclusions

The aim of the present work is to shed light on the stability of H-6 Carbon, which seems to be confusing. We performed *ab-initio* DFT calculations for the optimization of H-6 Carbon structure, using two different functionals (LDA/CA and GGA/PBE), and increasing number of k-grid points and mesh cutoff value. According to our findings, optimizations leads either to H-6 Carbon structure or to diamond, without any convergence trend related to the increasing number of k-grid points or mesh cutoff value. Using a transition pathway, which linearly converts H-6 Carbon to diamond, we showed that there is not any energy barrier along this transition pathway for both functionals and consequently, H-6 Carbon is unstable converted spontaneously to diamond. This conclusion was verified by a phonon band structure calculation on the H-6 optimized structure, which finds negative phonon frequencies.

On the other hand, performing TB calculations with the method used by Tamor and Hass[11], (which predicted that H-6 Carbon is stable), along the same transition pathway, we found that there is an overestimated energy barrier between H-6 Carbon and diamond and we showed that a much lower and more reliable barrier could be obtained by slightly modifying the cutoff function used.

Performing energy calculations of strained H-6 Carbon structures, we showed that the instability mechanism of H-6 Carbon is different from that of rhombohedral graphite, as suggested by Liu et al[12].

In order to understand the factors which are responsible for the H-6 Carbon instability, we combined the results obtained from the TB and the LDA calculations of H-6 Carbon along the transition pathway, with the results obtained using an hypothetical graphitic-like structure, which is formed from H-6 Carbon without rotation of the zig-zag chains. These calculations allowed us to express the energy as a sum of three contributions representing (i) the intrachain interactions of each zig-zag chain, (ii) the interchain interactions of the neighbouring zig-zag chains which are parallelly arranged and (iii) the strain induced interactions due to the rotation of the zig-zag chains. Using this analysis we found that the interchain and rotation contribution alone favour the conversion of H-6 Carbon to diamond, while the intrachain contribution does not (there is a barrier along the transition pathway). The sole combination of either the interchain or the rotation with the intrachain contribution can not eliminate that barrier but the combination of all three contributions can, making H-6 Carbon unstable. Therefore, the instability of H-6 Carbon is due to the synergetic action of both the rotation and the interchain contribution.

References

1 Z. G. Fthenakis and N. N. Lathiotakis, *Phys. Chem. Chem. Phys.*, 2015, **17**, 16418–16427.
2 A. N. Enyashin and A. L. Ivanovskii, *phys. stat. sol. (b)*, 2011, **248**, 1879–1883.
3 M. Côté, J. C. Grossman, M. L. Cohen and S. G. Louie, *Phys. Rev. B*, 1998, **58**, 664–668.
4 A. Y. Liu and M. L. Cohen, *Phys. Rev. B*, 1992, **45**, 4579–4581.
5 C. He, L. Sun, C. Zhang and J. Zhong, *Phys. Chem. Chem. Phys.*, 2013, **15**, 680–684.
6 J.-T. Wang, C. Chen, E. Wang and Y. Kawazoe, *Sci. Rep.*, 2014, **4**, 4339.
7 Z. Zhu, Z. G. Fthenakis, J. Guan and D. Tománek, *Phys. Rev. Lett.*, 2014, **112**, 026803.
8 A. Kuc and G. Seifert, *Phys. Rev. B*, 2006, **74**, 214104.
9 S. Zhang, Q. Wang, X. Chen and P. Jena, *Proc. Nat. Acad. Sci.*, 2013, **110**, 18809–18813.
10 J.-T. Wang, C. Chen and Y. Kawazoe, *Sci. Rep.*, 2013, **3**, 3077.
11 M. A. Tamor and K. C. Hass, *J. Mater. Res.*, 1990, **5**, 2273–2276.
12 A. Y. Liu, M. L. Cohen, K. C. Hass and M. A. Tamor, *Phys. Rev. B*, 1991, **43**, 6742–6745.
13 B. Winkler, C. J. Pickard, V. Milman and G. Thimm, *Chem. Phys. Lett.*, 2001, **337**, 36 – 42.
14 G.-M. Rignanese and J.-C. Charlier, *Phys. Rev. B*, 2008, **78**, 125415.
15 B. Zhang, *Comp. Mater. Sci.*, 2014, **82**, 540 – 543.
16 S. Fahy, S. G. Louie and M. L. Cohen, *Phys. Rev. B*, 1986, **34**, 1191–1199.
17 J. M. Soler, E. Artacho, J. D. Gale *et al.*, *J. Phys.: Cond. Matter*, 2002, **14**, 2745.
18 D. M. Ceperley and B. J. Alder, *Phys. Rev. Lett.*, 1980, **45**, 566–569.
19 J. P. Perdew and A. Zunger, *Phys. Rev. B*, 1981, **23**, 5048–5079.
20 J. P. Perdew, K. Burke and M. Ernzerhof, *Phys. Rev. Lett.*, 1996, **77**, 3865–3868.
21 N. Troullier and J. L. Martins, *Phys. Rev. B*, 1991, **43**, 1993–2006.
22 L. Kleinman and D. M. Bylander, *Phys. Rev. Lett.*, 1982, **48**, 1425–1428.
23 H. J. Monkhorst and J. D. Pack, *Phys. Rev. B*, 1976, **13**, 5188–5192.
24 J. C. Slater and G. F. Koster, *Phys. Rev.*, 1954, **94**, 1498–1524.
25 D. Tománek and S. G. Louie, *Phys. Rev. B*, 1988, **37**, 8327–8336.
26 Z. G. Fthenakis and D. Tománek, *Stretching graphite to diamond*, to be published.
27 Z. G. Fthenakis, *Mol. Phys.*, 2013, **111**, 3289–3296.

H-6 Carbon is unstable due to the synergetic action of the interchain interactions (U_{inter}) and the strain induced by the 60^{o} rotation of the zig-zag chains (U_{rot}), which eliminate the energy barrier provided by the intrachain interactions (U_{intra}) of H-6 Carbon, transforming H-6 Carbon to diamond.

H–6 Carbon → **Diamond**

λ=0 λ=0.5 λ=1

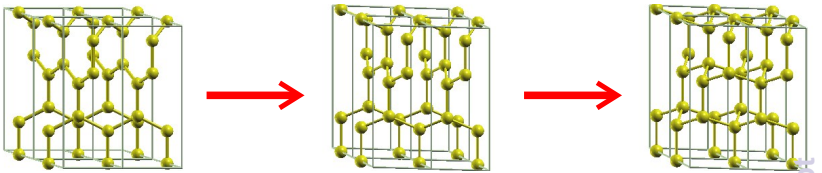

Energy components U of H–6 Carbon along the transition pathway converting H–6 Carbon to diamond.

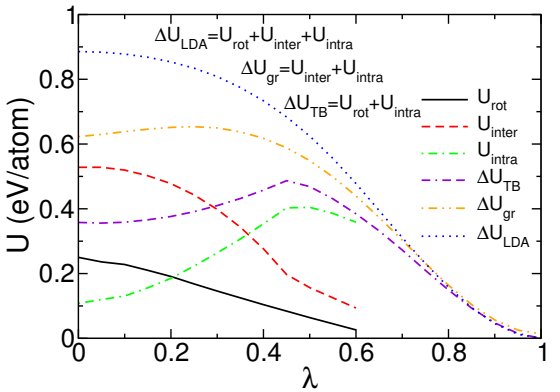

λ=0 λ=0.5 λ=1

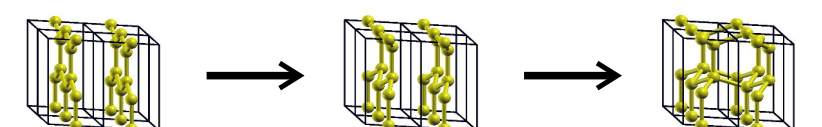

Graphitic–like → **Hex. Diamond**